Journal of Power Sources 196 (2011) 4270–4276

Contents lists available at ScienceDirect

Journal of Power Sources

journal homepage: www.elsevier.com/locate/jpowsour

Study of CO_2 stability and electrochemical oxygen activation of mixed conductors with low thermal expansion coefficient based on the $TbBaCo_3ZnO_{7+\delta}$ system

Vicente B. Vert, José M. Serra*

Instituto de Tecnología Química (Universidad Politécnica de Valencia – Consejo Superior de Investigaciones Científicas), Av. Naranjos s/n, E-46022 Valencia, Spain

ARTICLE INFO

Article history:
Received 4 August 2010
Received in revised form 8 November 2010
Accepted 8 November 2010
Available online 13 November 2010

Keywords:
CO_2 stability
Oxygen storage
SOFC
Cathode
Low thermal expansion

ABSTRACT

The influence of different application-oriented factors on the electrochemical activity and stability of $TbBaCo_3ZnO_{7+\delta}$ when used as a solid oxide fuel cell cathode has been studied. Calcination at temperatures above 900 °C (e.g. 1000 °C) leads to a significant increase in the electrode polarization resistance. The effect of the sintering temperature of the $TbBaCo_3ZnO_{7+\delta}$ cathode seems to be more important than the effect produced by the Tb substitution as observed when compared with 900 °C-sintered $YBaCo_3ZnO_{7+\delta}$; and $ErBaCo_3ZnO_{7+\delta}$ electrode performances. The presence of CO_2 in the air flow leads to an increase of roughly 10% in the polarization resistance for the whole studied temperature range (500–850 °C) while this effect is reversible. Analysis of the impedance spectroscopy measurements shows that the exchange rate constant (k_G from Gerischer element) is significantly affected by CO_2 at temperatures below 700 °C, while the diffusion coefficient related parameter is slightly influenced at low temperatures. Electrode degrades with a low constant rate of 1 $m\Omega\,cm^2\,h^{-1}$ after 60 h. This cathode material exhibits high CO_2 tolerance, as shown by temperature programmed treatment under a continuous gas flow of air with 5% CO_2, and a relatively low thermal expansion coefficient.

1. Introduction

Energy conversion on solid oxide fuel cells (SOFCs) systems used in stationary applications enables energy savings and high thermal integration. SOFC-based systems are an alternative for distributed energy production (combined power and heat generation) from fossil fuels (e.g. natural gas) and biomass-derived fuels (e.g. bioethanol) and are being introduced for building and domestic applications. However, high SOFC operating temperatures require the correct adjustment of the thermo-chemical properties of various cell components. Conventional SOFCs are based on oxygen-ion conducting electrolytes such as yttria-stabilized zirconia (8YSZ), or gadolinia, or samaria-doped ceria (GDC or SDC). The thermo-chemical properties of the other cell components should thus match those of the electrolyte material. For example, state-of-the art anodes are made of ceramic–metal composites (cermets) consisting of nickel oxide and the corresponding electrolyte material, i.e., 8YSZ or GDC. Cermet anode thermal expansion then correctly fits the electrolyte. Moreover, highly active cathode materials are based on cobaltites [1–4] containing lanthanides and strontium and have a perovskite crystalline structure. At high temperatures, the reactivity of these materials with conventional 8YSZ electrolyte is high [5] and it is necessary to apply a top GDC protective layer for SOFC applications [6]. In addition, perovskite materials based on cobaltites present significantly higher thermal expansion coefficients than the aforementioned electrolytes.

Recently, a series of materials based on the swedenborgite $YBaCo_4O_{7+\delta}$ structure have been described as oxygen-storage materials at high temperatures [7]. These layered cobalt oxide materials are related to the well-known $YBa_2Cu_3O_{7+\delta}$ superconductor [8,9]. This material exhibits a unique oxygen-storage behavior under atmospheric pressure and it is possible to achieve very high overstoichiometric values in oxygen at temperatures of around 325 °C. The $YBaCo_4O_{7+\delta}$ structure presents a hexagonal symmetry (space group $P6_3mc$) [10] and consists of two kinds of corner-sharing CoO_4 tetrahedra located in separate, alternatively stacked layers of triangular and kagome types. Cobalt cations are in tetragonal coordination and presumably the low-spin to high-spin transition may be inhibited [11], which could explain the relatively low thermal expansion coefficient experimentally determined for these materials. Moreover, yttrium cations are in octahedral coordination as a part of the kagome layer, and Ba cations are coordinated by 12 oxygen atoms. A weakness of this material is the low stability above 800 °C due to the reducibility of Co^{3+}. This aspect has been improved through: (1) the substitution of Y by other lanthanides with smaller ionic radii such as Yb and Lu [7,12]; and (2) the partial

* Corresponding author. Tel.: +34 963879448; fax: +34 963877809.
E-mail address: jsalfaro@itq.upv.es (J.M. Serra).

0378-7753/$ – see front matter © 2010 Elsevier B.V. All rights reserved.
doi:10.1016/j.jpowsour.2010.11.035

Nomenclature

R_{chem}	characteristic resistance ($\Omega\,cm^2$)
t_{chem}	characteristic relaxation time (s)
ω	frequency (Hz)
Z_0	Gerischer pseudo-impedance parameter ($\Omega\,cm^2\,s^{-0.5}$)
k_G	Gerischer rate constant parameter (s^{-1})
Γ	thermodynamic factor ($(1/2)((\partial \ln(pO_2))/\partial \ln(c_v))$)
A	surface area per volume ($cm^2\,cm^{-3}$)
k	oxygen surface exchange coefficient ($cm\,s^{-1}$)
c_i	oxide ion concentration ($mol\,cm^{-3}$)
c_v	oxygen vacancy concentration ($mol\,cm^{-3}$)
ε	electrode porosity
R	gas constant ($8.3145\,J\,K^{-1}\,mol^{-1}$)
T	temperature (K)
F	Faraday constant ($96{,}484\,C\,mol^{-1}$)
τ	electrode tortuosity
D_i	bulk diffusion coefficient of oxygen ions ($cm^2\,s^{-1}$)

substitution of Co by Zn (e.g. the compound $YBaCo_3ZnO_{7+\delta}$, achieves high stability above 900 °C) [13–15]. Preliminary tests have been made regarding the suitability of these materials as SOFC cathodes [16,17]. The interesting electrochemical behavior of these materials may be related to the reported oxygen mobility and storage capacity, and the important concentration of a redox catalytic metal such as cobalt. In [16], the electrochemical oxygen activation has been studied for three different compounds in which the lanthanide nature was varied while cobalt was partially substituted by zinc. In addition to the high electrochemical activity for oxygen activation, a low thermal expansion coefficient ($9.6 \times 10^{-6}\,K^{-1}$) that is very similar to that of state-of-the-art electrolyte materials has been confirmed.

This work has studied the influence on the electrochemical properties of $TbBaCo_3ZnO_{7+\delta}$ cathodes of: (1) sintering temperature with respect to the influence of other elements in the Tb position (e.g. Y or Er); (2) operation time; and (3) CO_2 presence in the cathode gas environment. For the last aspect, electrode polarization resistance of symmetrical cells has been recorded in CO_2-free and CO_2-containing air, including cycling between both atmospheres at 750 °C. Moreover, the possible reactivity of $TbBaCo_3ZnO_{7+\delta}$ with (1) 8YSZ and GDC (solid state reaction) and (2) CO_2 (carbonation reaction) in air at high temperatures during temperature-programmed experiments (TPA-MS) has been studied.

2. Experimental

Pellets made of pressed stoichiometric amounts of $BaCO_3$, $Co(CH_3COO)_2$, ZnO, and the corresponding anhydrous oxide (Tb, Er or Y) were calcined at 1200 °C for 12 h to obtain the cathode materials through solid state reaction. The starting precursor powders were previously mixed by ball-milling for 15 h in acetone. Single phase compounds were obtained for all sample compositions as confirmed by X-ray powder diffraction patterns obtained in a PANalytical X'Pert PRO diffractometer, using Cu $K\alpha_{1,2}$ radiation and an X'Celerator detector in a Bragg-Brentano geometry. The as-calcined cathode powders were milled with 3YSZ balls (Tosoh) in acetone after the particle size was homogenized by grinding in a mortar. Three roll mill (Exakt) was used to mix the milled powders with a terpineol–ethyl cellulose (6 wt.%) mixture. Refined screen-printable inks were applied on both sides of dense ~1 mm-thick 20 mol%-gadolinium doped ceria (GDC) disks and these were finally calcined in air at 900 °C for 2 h. The final electrode thickness is 30 μm. Symmetrical cells were tested by electrochemical AC impedance spectroscopy (EIS) using a 0 V DC – 50 mV AC signal in a $0.01–3 \times 10^5$ Hz frequency range in a Solartron 1470E+1455A FRA. EIS data was collected using a two-point configuration. Measurements were performed in the range from 500 to 850 °C. CO_2 was added to study the electrochemical stability of the electrodes against carbonation. After electrochemical analysis, fracture cross-sections of cells were analyzed by SEM using a JEOL JSM6300 microscope. Additionally, a mass spectrometer Omnistar (Balzers) was used for monitoring the evolution of the CO_2 signal of powdered samples following a heating ramp of 10 K min^{-1} up to 950 °C. Reference $Ba_{0.5}Sr_{0.5}Co_{0.8}Fe_{0.2}O_{3-\delta}$ (BSCF) powder was provided by IKTS Fraunhofer (Germany).

3. Results and discussion

3.1. Electrochemical results

3.1.1. Influence of sintering temperature

Fig. 1 (squares) presents the polarization resistance recorded for $TbBaCo_3ZnO_{7+\delta}$ cathodes sintered at 900 and 1000 °C in an Arrhenius arrangement. The increase in sintering temperature has a detrimental effect on the cathode performance and a fivefold rise in polarization resistance for the whole temperature range (500–850 °C) was observed. For both Tb-based electrodes, a change in the activation energy around 750 °C was observed and this is related to a change in the oxygen stoichiometry, as suggested by thermogravimetric measurements [16]. Specifically, at temperatures above 750 °C the material incorporates oxygen gradually and at temperatures close to 900 °C a steep oxygen release is observed and this may be related to a phase transition. Despite the significant resistance increase due to the higher cathode sintering temperature, a relevant change in the activation energy of the Tb-based electrodes at high temperatures was not observed, (i.e., activation energy is slightly higher for the electrode sintered at 1000 °C, while at low temperatures the activation energy is nearly the same (1.1 eV) irrespective of the cathode sintering temperature). Therefore, it seems that the electrochemical activity of both Tb-containing electrodes is limited by similar processes in the 500–750 °C range. This is also supported by the impedance spectroscopy measurements, which do not show relevant changes in the processes at different frequencies (Fig. 2). At high temperatures (Fig. 2a – 850 °C) for both Tb electrodes, the rate limiting processes are associated with medium-to-high frequency processes (relaxation times around 1–10 kHz), which might be related to transport

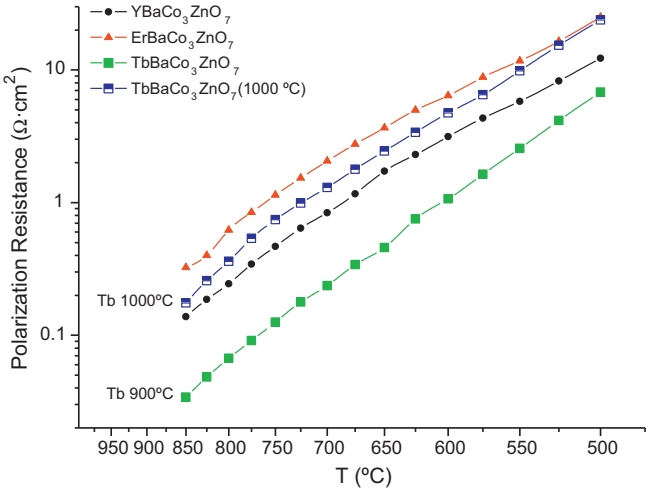

Fig. 1. Arrhenius plot of the polarization resistance for Tb-based electrode sintered at 900 and 1000 °C, and the electrodes based on Y and Er sintered at 900 °C.

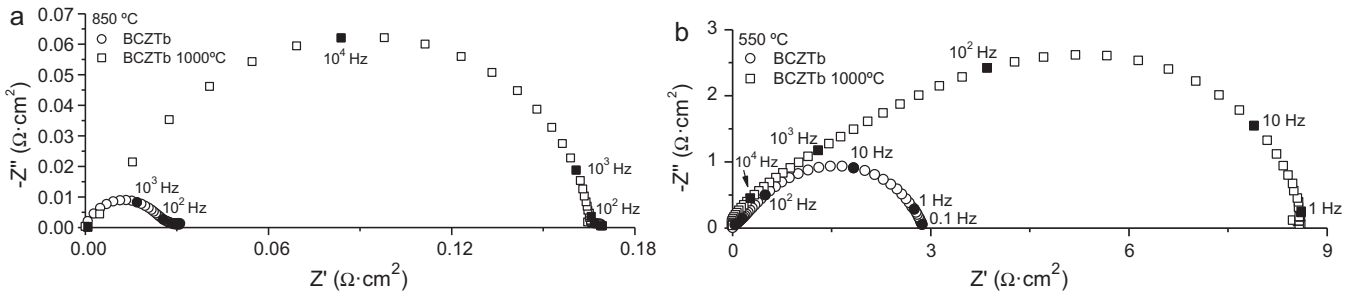

Fig. 2. Nyquist plots for $TbBaCo_3ZnO_{7+\delta}$ sintered at 900 °C (circles) and 1000 °C (squares). Operation temperature is 850 °C (a) and 550 °C (b). Frequency decades are indicated as solid symbols.

processes through the electrode and electrode–electrolyte interfaces. However, at intermediate temperatures, e.g. 550 °C (Fig. 2b), the limiting processes are related to low frequencies (relaxation times around 10 Hz), which are typically ascribed [18] to coupled surface reaction and electrode oxygen-ion diffusion in mixed ionic–electronic conductors. For both temperature ranges, the rate limiting processes are slightly shifted to higher frequencies when the sintering temperature increases, i.e., raising the polarization resistance. Nevertheless, the indications obtained through the analysis of frequency ranges should be confirmed by deeper impedance analysis with model electrodes and (oxygen-ion) transport studies. These analyses have not yet been made for this novel type of cathode material. In Fig. 1, the polarization resistance corresponding to two electrodes based on Er and Y sintered at 900 °C is plotted. It is remarkable that the effect of the change in sintering temperature is much more important than the change of the lattice composition. Er- and Y-based electrodes show similar activation energy levels at high temperatures to the Tb-based samples sintered at 1000 °C. However, at low temperatures the activation energy level is somewhat lower (~0.8 eV) with respect to both Tb-based electrodes (~1.1 eV).

Fig. 3 presents SEM images of the fractured cross-section of the four electrodes studied in Fig. 1. All three electrodes sintered at 900 °C show a similar microstructure comprising two particle size distributions, i.e., comprising large (1–3 μm) and small particles (below 0.5 μm). The small particles dispersed on the large particles make a higher surface area available for oxygen reduction. The small particles are not visible for the electrode treated at 1000 °C and this is ascribed to the high sintering activity of this kind of material – especially for nanosized particles. The reduction of surface area may partly explain the inferior electrochemical behavior of this electrode. Moreover, the occurrence of cathode–electrolyte

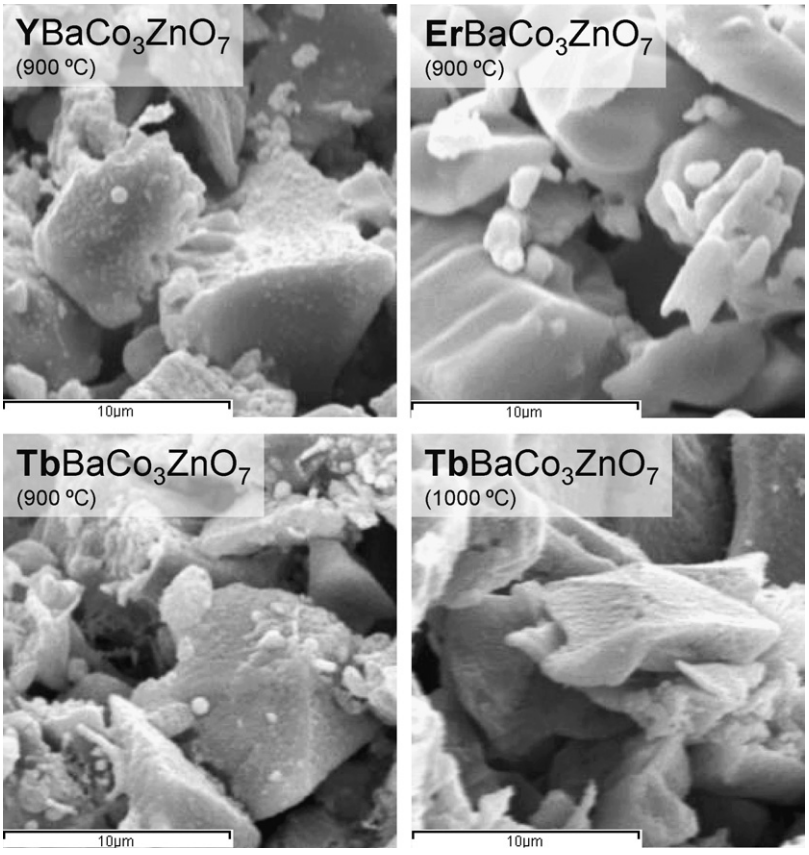

Fig. 3. SEM micrographs of the fracture cross-section of Tb-based electrode sintered at 900 °C and 1000 °C, and the electrodes based on Y and Er sintered at 900 °C after electrochemical testing.

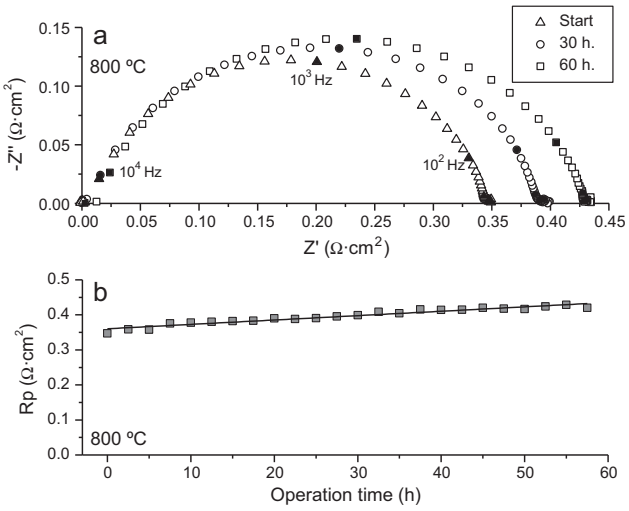

Fig. 4. Time stability of $TbBaCo_3ZnO_{7+\delta}$ electrode sintered at 900 °C. (a) Nyquist plot for measurements at 0, 30, and 60 h at 800 °C (frequency decades are indicated as solid symbols); and (b) time evolution of the polarization resistance at 800 °C.

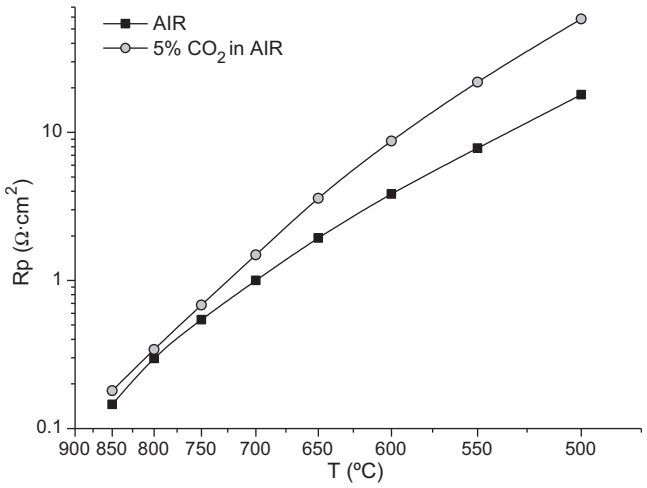

Fig. 5. Arrhenius plot of the polarization resistance for Tb-based electrode sintered at 900 °C under air and air with CO_2 (5 vol.%).

interfacial limitations related to possible reaction or interdiffusion processes during sintering at higher temperatures cannot be excluded. The detection of new interfacial phases could not be ascertained by XRD analysis (see Section 3.2.1).

3.1.2. Influence of operation time

The time degradation of the electrochemical activity of the electrode $TbBaCo_3ZnO_{7+\delta}$ sintered at 900 °C is evaluated in this section. Electrochemical impedance spectra have been recorded at 800 °C under constant air flow for more than 60 h. Fig. 4a shows the initial, intermediate, and final recorded impedance spectra. After 60 h the total impedance increased only 65 $m\Omega\,cm^2$ and this corresponds to a degradation rate of 1 $m\Omega\,cm^2\,h^{-1}$. The degradation rate is low for such a Co-rich compound at 800 °C, especially when considering the poor stability at high temperatures of the parent compound $YBaCo_4O_{7+\delta}$. The zinc partial substitution of cobalt and the use of terbium increase stability at high temperatures. The corresponding polarization resistance values are plotted versus time in Fig. 4b. Polarization resistance increases with time, although the degradation rate is low (see the *x*-axis scaling). However, the degradation process apparently does not affect the limiting processes as shown when comparing the frequency evolution (notice the decades) of the Nyquist plot in Fig. 4a.

3.1.3. CO_2 effect on electrochemical behavior

The high oxygen storage capability of $TbBaCo_3ZnO_{7+\delta}$ and other element-substituted (Er or Y) materials makes these compounds suitable for both SOFC cathode and oxygen separation membrane applications. The cell volume expansion analysis [16] confirms the stability of the swedenborgite structure at high temperatures in an oxygen partial pressure (pO_2) range from 1 to 10^{-5} atm. Moreover, no chemical expansion has been detected in the crystalline structure in the studied pO_2 range – while an anisotropic thermal behavior related to the layered nature of this structure was observed. However, a critical issue for Ba-rich compounds, such as BSCF [19–21], is the detrimental effect that CO_2-containing atmospheres have on the (electrochemical) surface oxygen activation and crystal stability – leading to decomposition through carbonation processes. CO_2 stability is an important aspect for application as single chamber SOFC cathode and also for application as a SOFC cathode in a classical configuration, since air contains ca. 380 ppm of CO_2 and the sensitivity of BSCF, even at 300 ppm [22], has been described. The effect on the electrochemical behavior was studied on a $TbBaCo_3ZnO_{7+\delta}$ symmetrical cell by recording impedance spectra from 850 to 500 °C under air with CO_2. Specifically, after treatment under synthetic air, the temperature was again raised to 850 °C and then the gas flow was changed to a 5% CO_2-containing air flow (20% O_2, N_2 balance). The polarization resistance under both atmospheres is presented in Fig. 5 (Arrhenius plot). The negative effect of CO_2 on the electrode operation is important at low temperatures; while at high temperatures (750–850 °C) there is only a minor effect. Since the rate limiting step at low temperatures (500–600 °C) has been previously associated to low frequency processes, i.e., surface related processes, it may be concluded that the presence of CO_2 principally affects the surface processes. Specifically, a strong adsorption of CO_2 on the barium cations accessible on the material surface [23] is expected, and therefore the surface oxygen coverage is diminished and this results in a net decrease of the oxygen reduction rate. Moreover, it is reasonable to assume that the CO_2 may not much influence the oxygen-ion diffusion through the electrode bulk. Additionally, the specific rate limiting mechanism is somehow slightly altered as concluded from the small increase in the apparent activation energy under the CO_2-containing gas at low temperatures. Furthermore, two different activation energy ranges are still present for both measurements in synthetic air and CO_2-containing air – although the transition temperature has changed under CO_2-containing air. In the high temperature regime, the activation energy is kept almost constant. The resistance due to adsorption hindrance introduced by CO_2 is significant at temperatures below the transition temperature.

Nyquist plots of the collected impedance data (e.g. Fig. 2b) show a particular shape corresponding to a Gerischer process [24,25]. Proper fitting of this data enables a better understanding of the CO_2 effect on electrode processes. From the Gerischer model two parameters can be extracted and compared. In Fig. 6 the rate constant (k_G) and the Gerischer pseudo-impedance (Z_0) are plotted in an Arrhenius arrangement. The rate constant can be related to the surface exchange coefficient for oxygen reduction reaction. The pseudo-impedance is indicative of the oxygen diffusion through the bulk material.[1] The competitive adsorption [26] between O_2 and CO_2 means that in CO_2-containing air the rate constant values are lower than in the air as depicted in Fig. 6a. This difference becomes

[1] $k_G = \frac{1}{t_{chem}} = \frac{\Gamma \cdot A \cdot k \cdot c_i}{(1-\varepsilon)\cdot c_V} \propto k.$

$Z_0 = R_{chem} \cdot \sqrt{k_G} = \frac{RT}{2 \cdot c_i \cdot F^2} \sqrt{\frac{\Gamma \cdot \tau \cdot c_i}{(1-\varepsilon)\cdot c_V \cdot D_i}} \propto D_i^{-0.5} \rightarrow Z_0^{-2} \propto D_i.$

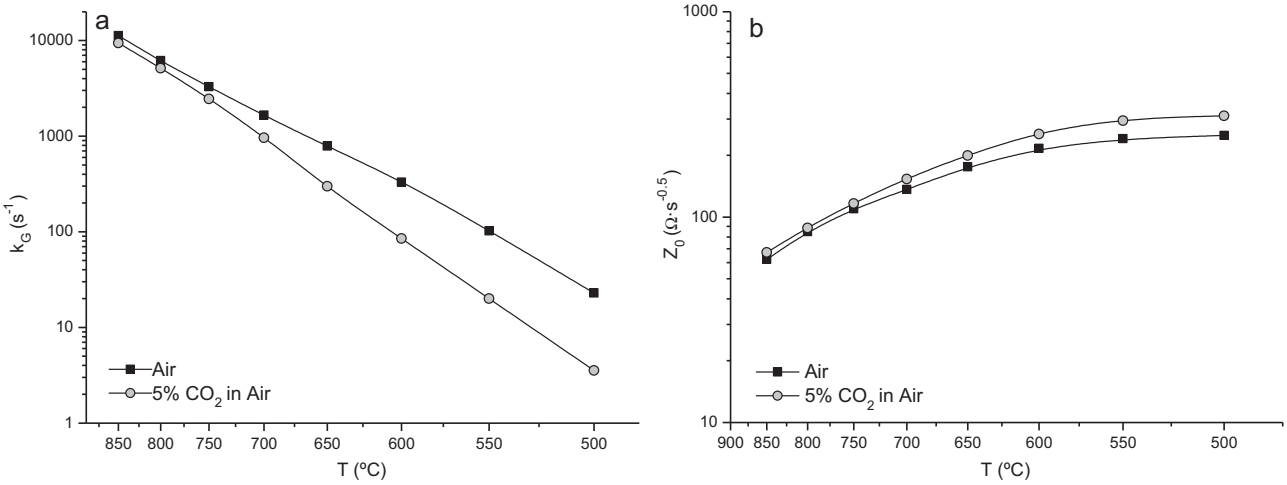

Fig. 6. Arrhenius plot of the Gerischer parameters (exchange rate k_G and pseudo-impedance Z_0) for Tb-based electrode sintered at 900 °C under air (squares) and air with 5 vol.% CO_2 (circles).

greater as the temperature is lowered since the surface processes are becoming more dominant. The pseudo-impedance variation is unimportant and only a slight increase is observed at temperatures below 600 °C. This fact could be related to a limitation in the surface oxygen-ion diffusion towards the electrolyte caused by CO_2 adsorption and possible changes in the oxygen lattice content due to the environmental change. The apparent activation energy for pseudo-impedance both in air and CO_2-air changes abruptly around 650 °C. The rise in temperature and CO_2 surface coverage leads to structural and local oxygen stoichiometry changes, which may have an influence on oxygen-ion diffusion.

To determine the reversibility of the CO_2 effect on electrochemical activity, a series of cycles between air and CO_2-containing air were made using the symmetrical cell configuration. The selected temperature was 750 °C in order to enable the possible formation of carbonates. Impedance spectra have been recorded at different times during gas environment cycling. This cycling process is shown in Fig. 7, where the polarization resistance values are plotted as a function of time. As previously stated, the addition of CO_2 to the air flow increases the electrode polarization resistance while the time evolution indicates a progressive degradation, i.e., a resistance increase. However, when fresh air is fed again, the electrochemical response is very fast and the original electrochemical activity

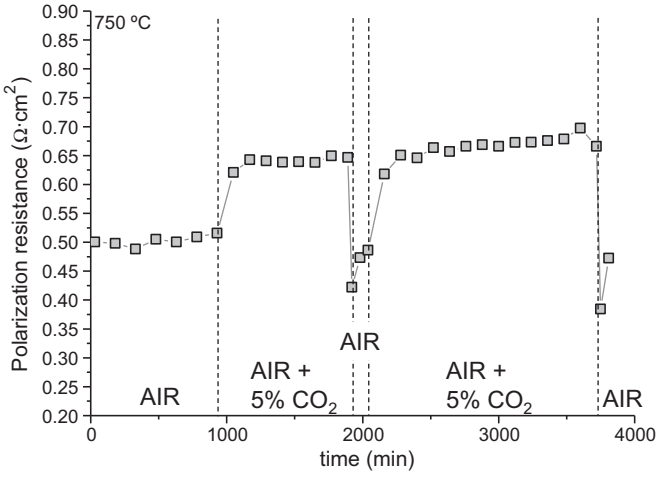

Fig. 7. Effect of CO_2 and CO_2/air cyclability on the polarization resistance for Tb-based electrode sintered at 900 °C under air and air with 5 vol.% CO_2.

is totally recovered. A new CO_2 cycle shows that the activity loss is even higher, albeit that the initial polarization resistance is fully recovered after shifting again to fresh air. The cycling shows (1) the reversible effect of CO_2; and (2) that the CO_2-related degradation rate is low (note the small resistance scale in Fig. 7). The progressive detrimental effect of CO_2 cannot be related to the degradation of the crystalline phase; but to the adsorption process and lattice oxygen stoichiometric changes. In fact, this electrode material shows a rather complex oxygen incorporation/loss which is very sensitive to pO_2 changes [16].

3.2. Chemical compatibility and reactivity

3.2.1. Reactivity with electrolyte materials

Commercially available electrolyte materials were mixed with Tb-based material. 8YSZ from Aldrich and GDC from Treibacher were first analyzed by XRD at room temperature and compared with the XRD pattern of the Tb-based material. A mixture (50 wt.%) of this Tb-material with the aforementioned electrolytes was prepared by grinding it in a mortar. The mixed powders were checked by XRD prior to calcination at 1150 °C for 10 h. Fig. 8 shows the XRD analyses. The reactivity with 8YSZ is evident after thermal treatment. Some unidentified diffraction peaks appear (* symbols in Fig. 8a) after 10 h at 1150 °C in the XRD spectra of the calcined 8YSZ-Tb mixture – while other diffraction peaks (+ symbols) disappeared after thermal treatment. GDC electrolyte material seems to be a good candidate for the $TbBaCo_3ZnO_{7+\delta}$ cathode material. No peaks other than the original two phases are observed after the high temperature treatment for the mixed powders as shown in Fig. 8b. Therefore, $TbBaCo_3ZnO_{7+\delta}$ seems to be compatible with GDC electrolyte since there is apparently no solid state reaction (to the limits of XRD analysis) after treatment under manufacturing-like conditions. Moreover, the electrochemical testing carried out on GDC electrolytes showed notable time stability and relatively low polarization resistance, in which the resistance corresponding to the interface GDC-$TbBaCo_3ZnO_{7+\delta}$ is included.

3.2.2. Stability against carbonation

This section presents a further investigation of CO_2 stability by means of temperature-programmed CO_2 consumption experiments. A fixed bed of the material was exposed to a continuous gas flow of CO_2 (5 vol.%) in air under a constant heating rate; and the outlet CO_2 concentration was monitored by

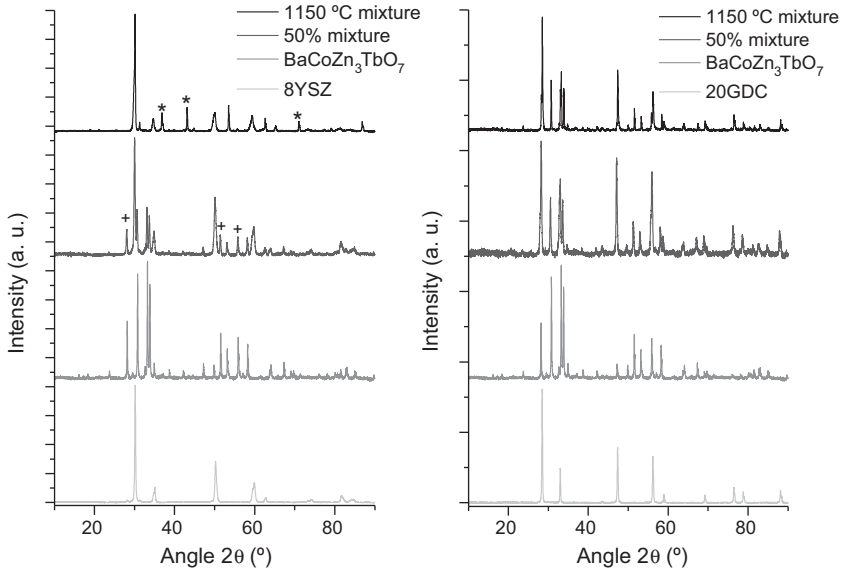

Fig. 8. Compatibility study with electrolyte materials (8YSZ and GDC). XRD patterns of the electrode $TbBaCo_3ZnO_{7+\delta}$ and electrolyte materials before and after treatment at 1150 °C for 10 h (* symbols denote new unidentified peaks and + symbols denote peaks absent after heat treatment).

mass spectrometry (MS). Fig. 9 shows the evolution of the CO_2 concentration as a function of temperature for two different materials $Ba_{0.5}Sr_{0.5}Co_{0.2}Fe_{0.8}O_{3-\delta}$ (BSCF) and $TbBaCo_3ZnO_{7+\delta}$. BSCF has been selected as a reference material since it contains important amounts of barium and cobalt and this compound has shown a very high ionic conductivity and oxygen activation rate. BSCF shows a significant CO_2 uptake in the temperature range between 350 and 780 °C while CO_2 is released at high temperatures. It is well known that BSCF decomposes in the observed temperature range to form mixed Ba–Sr carbonates and other Fe–Co mixed and single oxides [23]. At temperatures above 800 °C carbonates decompose although the original perovskite structure is not recovered. However, $TbBaCo_3ZnO_{7+\delta}$ shows very little CO_2 uptake and releases small amounts of CO_2 at temperatures of around 830 °C. CO_2 uptake and release may be linked principally to surface adsorption, since the swedenborgite structure is maintained for the whole temperature range and the presence of carbonates could not be detected by XRD analysis.

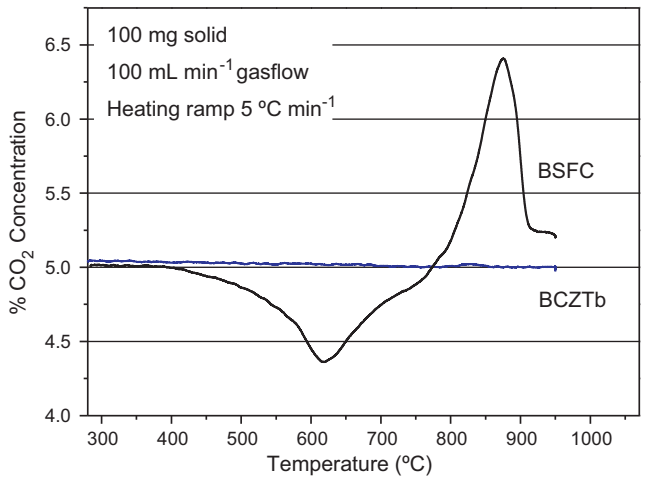

Fig. 9. Temperature programmed CO_2-uptake/release experiment for BSCF and $TbBaCo_3ZnO_{7+\delta}$.

4. Conclusions

Different aspects of the electrochemical activity and stability of $TbBaCo_3ZnO_{7+\delta}$ have been studied in order to assess its applicability as a SOFC cathode. The sintering temperature of the cathode layer on the electrolyte is very critical and the change from 900 °C to 1000 °C results in a significant increase in electrode polarization resistance. The effect of the sintering temperature is more decisive than the effect produced by the substitution of the lanthanide, as observed for three different tested substituting elements (Tb, Y, and Er). 5%-CO_2 containing air atmospheres lead to an increase of about 10% in the polarization resistance for the whole studied temperature range of 500–850 °C). This effect is reversible although the CO_2 exposure lasted for several hours. Specifically, the effect of CO_2 is related to surface processes, i.e., surface adsorption and competition with oxygen and this is concluded on the basis of the impedance measurement analysis (Gerischer element fitting). It was observed that the surface exchange rate is notably influenced by CO_2 at temperatures below 700 °C while the parameter related to the diffusion coefficient is slightly affected at low temperatures. The electrode showed a low degradation rate of 1 $m\Omega\,cm^2\,h^{-1}$ after testing for 60 h. With respect to chemical compatibility with electrolyte materials, the solid state reaction with 8YSZ at 1150 °C for 10 h was observed – while no reaction with GDC was observed to the limits of XRD analysis. Moreover, $TbBaCo_3ZnO_{7+\delta}$ exhibits a high CO_2 tolerance (as shown by temperature programmed treatment under a continuous gas flow of air with 5% CO_2) in combination with a relatively low expansion coefficient, despite the high barium and cobalt content of this material.

Acknowledgements

Financial support by the Universitat Politècnica de València (Grant UPV-2007-06), the Spanish Ministry for Science and Innovation (Project ENE2008-06302), the EU through FP7 NASA-OTM Project (NMP3-SL-2009-228701), and the Helmholtz Association of German Research Centres through the Helmholtz Alliance MEMBRAIN (Initiative and Networking Fund) is kindly acknowledged.

The revision of this paper was funded by the Politècnica de València. The authors wish to thank S. Jiménez for material preparation.

References

[1] J.M. Serra, V.B. Vert, ChemSusChem 2 (2009) 957.
[2] A. Esquirol, N.P. Brandon, J.A. Kilner, M. Mogensen, J. Electrochem. Soc. 151 (2004) A1847.
[3] A. Mai, V.A.C. Haanappel, S. Uhlenbruck, F. Tietz, D. Stöver, Solid State Ionics 176 (2005) 1341.
[4] J.M. Serra, H.-P. Buchkremer, J. Power Sources 172 (2007) 768.
[5] E.V. Tsipis, V.V. Kharton, J. Solid State Electrochem. 12 (2008) 1367.
[6] J.M. Serra, V.B. Vert, M. Betz, V.A.C. Haanappel, W.A. Meulenberg, F. Tietz, J. Electrochem. Soc. 155 (2008) B207.
[7] S. Kadota, M. Karppinen, T. Motohashi, H. Yamauchi, Chem. Mater. 20 (2008) 6378.
[8] M.K. Wu, J.R. Ashburn, C.J. Torng, P.H. Hor, R.L. Meng, L. Gao, Z.J. Huang, Y.Q. Wang, C.W. Chu, Phys. Rev. Lett. 58 (1987) 908.
[9] F. Tietz, A. Arul Raj, W. Jungen, D. Stöver, Acta Mater. 49 (2001) 803.
[10] M. Valldor, M. Andersson, Solid State Sci. 4 (2002) 923.
[11] M.A. Señarís-Rodrígez, J.B. Goodenough, J. Solid State Chem. 118 (1995) 323.
[12] N. Nalayama, T. Mizota, Y. Ueda, A.N. Sokolov, A.N.N. Vasiliev, J. Magn. Mater. 300 (2006) 98.
[13] H. Hao, X. Zhang, Q. He, Ch. Chen, X. Hu, Solid State Commun. 141 (2007) 591.
[14] H. Hao, L. Zhao, X. Hu, H. Hou, J. Therm. Anal. Calorim. 95 (2009) 585.
[15] M. Valldor, Solid State Chem. 6 (2004) 251.
[16] V.B. Vert, J.M. Serra, J.L. Jordá, Electrochem. Commun. 12 (2010) 278.
[17] J. Kim, A. Manthiram, Chem. Mater. 22 (2010) 822.
[18] S.B. Adler, Chem. Rev. 104 (10) (2004) 4791.
[19] M. Arnold, H. Wang, A. Feldhoff, J. Membr. Sci. 293 (2007) 44.
[20] Z. Yang, A.S. Harvey, L.J. Gaukler, Scripta Mater. 61 (2009) 1083.
[21] J. Peña-Martinez, D. Marrero-Lopez, J.C. Ruiz Morales, P. Nuñez, C. Sanchez-Bautista, A.J. Dos Santos-Garcia, J. Canales-Vazquez, Int. J. Hydrogen Energy 34 (2009) 9486.
[22] J.H. Park, J.P. Kim, S.H. Son, Energy Proc. 1 (2008) 369.
[23] K. Nomura, Y. Ujihira, T. Hayakawa, K. Takehira, Appl. Catal. B: Gen. 137 (1996) 25.
[24] B.A. Boukamp, H.J.M. Bowmeester, Solid State Ionics 157 (2003) 29.
[25] S.B. Adler, J.A. Lane, B.C.H. Steele, J. Electrochem. Soc. 143 (1996) 3554.
[26] A. Yan, B. Liu, Y. Dong, Z. Tian, D. Wang, M. Cheng, Appl. Catal. B: Environ. 80 (2008) 24.